Current Research in Parasitology & Vector-Borne Diseases 4 (2023) 100153

Contents lists available at ScienceDirect

Current Research in Parasitology & Vector-Borne Diseases

journal homepage: www.sciencedirect.com/journal/current-research-in-parasitology-and-vector-borne-diseases

Extracellular vesicles of the liver fluke *Opisthorchis felineus* stimulate the angiogenesis of human umbilical vein endothelial cells

Dmitry V. Ponomarev [a], Ekaterina A. Lishai [a], Anna V. Kovner [a], Maria V. Kharkova [b], Oxana Zaparina [a], Yaroslav K. Kapuschak [a], Viatcheslav A. Mordvinov [a], Maria Y. Pakharukova [a,c,d,*]

[a] Institute of Cytology and Genetics (ICG), Siberian Branch of the Russian Academy of Sciences (SB RAS), 10 Akad. Lavrentiev Ave., Novosibirsk, 630090, Russia
[b] Institute of Chemical Biology and Fundamental Medicine, Siberian Branch of the Russian Academy of Sciences, 8 Akad. Lavrentiev Ave., Novosibirsk, 630090, Russia
[c] Department of Natural Sciences, Novosibirsk State University, 2 Pirogova Str., Novosibirsk, 630090, Russia
[d] Institute of Molecular Biology and Biophysics of Federal Research Center of Fundamental and Translational Medicine, 2 Timakova Str., Novosibirsk, 630117, Russia

ARTICLE INFO

Keywords:
Extracellular vesicles
Helminth
Opisthorchis felineus
Transcriptome
Human vascular endothelial cells

ABSTRACT

The liver fluke *Opisthorchis felineus* is a clinically important food-borne parasite of humans. Infection with *O. felineus* in mammals is associated with liver morbidities such as periductal fibrosis, bile duct neoplasia, and chronic inflammation. Previously we have shown that excretory-secretory products (ESP) can stimulate the healing of skin wounds in mice, which may be due to stimulated angiogenesis and extracellular matrix remodeling. However, there are no studies analyzing the angiogenic character of *O. felineus*, and its effects on angiogenesis, vascularity, and vascular endothelium. The aim of this study was to evaluate the capacity of ESP and extracellular vesicles (EVs) of *O. felineus* to stimulate angiogenesis and the formation of pseudo-capillaries *in vitro*. We also aimed at the assessment of the angiogenesis during the infection *in vivo*, and estimation of the endothelial cell type abundances from heterogeneous bulk liver transcriptome between uninfected and infected animals with single-cell information. The study revealed significant alterations in vascularity in the hamster liver and significant involvement of portal endothelial cells at the transcriptome level. We also demonstrated that the ESP and EVs of *O. felineus* have the capacity to stimulate the formation of pseudo-capillaries *in vitro*. Both ESP and EVs appeared to have similar effects on all four parameters, increasing node formation and total master segments length, and significantly decreasing total isolated branches length and number of isolated segments of pseudo-capillaries. The liver flukes manipulate the host's angiogenic response, a fact that has been related to the pathogenesis caused by these parasites. Understanding these pathogenic mechanisms may uncover new therapeutic targets to relieve or prevent the most severe complications of opisthorchiasis.

1. Introduction

The liver fluke *Opisthorchis felineus* (Rivolta, 1884) is a widespread fish-borne trematode, one of clinically important food-borne parasites (FAO/WHO, 2014). *Opisthorchis felineus* occurs throughout eastern Europe and Russia and also in western Europe (Pozio et al., 2013; Scaramozzino et al., 2018). Infection of mammals occurs after ingestion of raw or undercooked freshwater cyprinid fishes infected with the larval stage, the metacercaria. Natural foci of opisthorchiasis are active and tend to expand (Pakharukova and Mordvinov, 2016, 2022).

Adult worms parasitize the biliary tract of mammals, including humans, and cause damage to the hepatobiliary system, with some serious complications. The disease involves chronic inflammation, inflammatory infiltrates, egg granulomas, and periductal fibrosis within the portal tract of the liver (Pakharukova et al., 2019a, b). It is known that many helminths are characterized by the stimulation of neoangiogenesis in the organs they parasitize, contributing to disturbances of vascularity and pathological changes of blood vessels, which contribute to the pathogenesis (Andrade et al., 2006; Hamed et al., 2006; Shirai et al., 2006; Dennis et al., 2011; Hasby Saad and El-Anwar, 2020). Investigation of the factors that can affect host angiogenesis has shown that proangiogenic factors can probably be contained in schistosome

* Corresponding author. Institute of Cytology and Genetics (ICG), Siberian Branch of the Russian Academy of Sciences (SB RAS), 10 Akad. Lavrentiev Ave., Novosibirsk, 630090, Russia.
E-mail address: pmaria@yandex.ru (M.Y. Pakharukova).

https://doi.org/10.1016/j.crpvbd.2023.100153
Received 30 June 2023; Received in revised form 5 October 2023; Accepted 26 October 2023
Available online 7 November 2023

eggs (Mbanefo et al., 2020) or secreted as excretory-secretory products (ESPs) or extracellular vesicles (EVs) (Kifle et al., 2020; Pérez Rodríguez et al., 2023). For instance, recombinant *O. viverrini* granulin (rOV-GRN-1) stimulates angiogenesis (Haugen et al., 2018).

Numerous recent studies indicate that parasite-derived EVs play a variety of regulatory roles during infection. It has been shown that many helminth species, including *O. felineus*, can secrete EVs (Pakharukova et al., 2023). It has also been demonstrated that these EVs can be taken up by human cells, such as cholangiocytes (Pakharukova et al., 2023), human umbilical vein endothelial cells (HUVECs), or THP1 monocytes (Kifle et al., 2020). Preliminary data suggest that the secretory products of *O. felineus* can stimulate the healing of skin wounds in mice, and this effect may be due to stimulated angiogenesis and extracellular-matrix remodeling (Kovner et al., 2022). However, there are no studies on the angiogenic nature of *O. felineus* or its effects on angiogenesis, vascularity, or a vascular endothelium.

The aim of this study was to assess the influence of *O. felineus* infection on angiogenesis *in vivo* and to accurately determine abundance levels of endothelial cell types from the heterogeneous bulk liver transcriptome. In addition, we aimed to evaluate the capacity of secretory products and EVs of *O. felineus* to stimulate angiogenesis and the formation of pseudo-capillaries *in vitro*.

2. Materials and methods

2.1. Sample collection and histochemistry

Male Syrian hamsters aged 6–8 weeks were used and infected each orally with 50 metacercariae of *O. felineus*. The hamsters (12 animals) were housed individually and euthanized using carbon dioxide at 12 weeks post-infection (p.i.).

Liver samples collection and histochemistry was performed as described previously (Pakharukova et al., 2019b; Mordvinov et al., 2021; Kovner et al., 2022). The resulting paraffin sections were stained *via* a standard protocol with Congo-red stain (Labiko, Saint Petersburg, Russia) (amyloid stains orange-red). The visualization of staining-positive blood vessels was carried out under an AxioImager A1 microscope (Zeiss, Jena, Germany) equipped with an AxioCam MRc camera (Zeiss).

2.2. Cell culture and parasites

HUVECs were isolated and cultivated as fully described previously (Stepanova et al., 2019). Adult parasites were recovered from the bile ducts of hamsters infected with 50 metacercariae of *O. felineus*. Adult parasites were washed 10 times in sterile saline. Production of EVs or ESP was initiated on Day 2, and parasites were maintained in RPMI 1640 supplemented with 1% of glucose and 100 μg/ml penicillin-streptomycin (Sigma-Aldrich, Burlington, USA) and amphotericin B.

2.3. Isolation of exosome-like vesicles (EVs) and ESP

ESP and EVs were isolated from the conditioned medium of 300 adult parasites maintained for 72 h in 6-well culture plates (30–40 parasites per well) according to a previously published protocol (Kovner et al., 2022; Pakharukova et al., 2023). Complete protease inhibitor cocktail (Abcam, Boston, USA) was added to the resuspended EVs and to the concentrated ESP. EVs and ESP were aliquoted and stored at −80 °C. The protein content of the ESP and EVs was quantified by the BCA assay (Thermo Fisher Scientific, Waltham, USA) according to the manufacturer's recommendations. The resulting EVs pellet was confirmed to consist of vesicles of 40–150 nm in size by transmission electron microscopy.

2.4. Bioinformatics analysis

The following gene expression datasets were used: the hamster liver transcriptome (intact) and the liver transcriptome of hamsters infected with *O. felineus* at 1 and 3 months p.i. (NCBI: SRX13451950-SRX13451961). Sequence mapping to the genome of the golden hamster BCM_Maur_2.0 (2021) was performed using the STAR software (v.2.7.10b). Differential gene expression was analyzed by the Wald test (with a threshold of 0.05) from the R package *DESeq2* (v.1.38.3) (Love et al., 2014). The probability values obtained after the analysis were corrected for multiple comparisons (Benjamini-Hochberg) and genes were defined as differentially expressed at $P_{adj} < 0.05$ and a gene expression change > 2-fold. Weakly expressed genes were removed from the expression matrix (the sum of gene expression values for all libraries was less than 47).

Pathway enrichment analysis was performed by means of the Kyoto Encyclopedia of Genes and Genomes (KEGG) and Molecular Signatures Database (MsigDB: curated and hallmark gene sets) based on mouse genome annotation (R package *msigdb* (v.1.6.0)). The R package *clusterProfiler* (v.4.6.2) was used for this analysis (Yu et al., 2012; Wu et al., 2021).

To accurately determine cell type abundance levels from heterogeneous bulk expression data of the liver, we applied the R package *BisqueRNA 1.0.5* and previously published human liver single-cell RNA sequencing (scRNA-seq) data (MacParland et al., 2018; Jew et al., 2020). A reference-based method was employed that utilizes single-cell information to generate a signature matrix and transformation of bulk expression data for accurate regression-based estimates.

2.5. Tube formation assay

HUVECs were cultured in the DMEM/F12 medium (Merck, Darmstadt, Germany) supplemented with 2% of FBS (Gibco, Thermo Fisher Scientific, Waltham, USA), 5 ng/ml recombinant human VEGF (rhVEGF) (PSG010-10, Sci-store, Moscow, Russia), 5 ng/ml rhFGF2 (PSG060-10, Sci-store, Russia), 15 ng/ml rhIGF-1 (PSG120-10, Sci-store, Russia), 5 ng/ml rhEGF (PSG130-10, Sci-store, Russia), 1 μg/ml hydrocortisone (H4001, Sigma-Aldrich, Burlington, USA), 1 mM L-glutamine (Biolot, Saint Petersburg, Russia), 7.5 U/ml heparin (Ozon Pharmaceuticals, Novosibirsk, Russia), and 50 μg/ml L-ascorbic acid (Sigma-Aldrich, Burlington, USA). The cells were passaged once per 3–4 days after 70–80% confluence was reached. To dissociate the cells, a 0.1% solution of collagenase IV was used.

For the tube formation assay, Matrigel (Corning, New York, USA) was diluted 1:1 with the medium and added into wells of a 96-well plate in the amount of 40 μl in accordance with the manufacturer's recommendations. After polymerization of the gel, the cells were seeded on Matrigel in a medium containing a reduced concentration of growth factors to set up a negative control with the lowest degree of formation of tubulo-like structures. This negative control medium was composed of DMEM/F12, 2% of FBS, 1.25 ng/ml rhVEGF, 1.25 ng/ml rhFGF2, 3.75 ng/ml rhIGF-1, 1.25 ng/ml rhEGF, 0.25 μg/ml hydrocortisone, 2.5 mM L-glutamine, 0.17 U/ml heparin, and 12.5 μg/ml L-ascorbic acid. Bovine serum albumin (BSA, Sigma, USA) was added as a non-specific control at a concentration of 32 μg/ml. Either the ESP at a concentration of 32 μg/ml or EVs at 10 μg/ml were added to the cells, and the gel plate was incubated at 37 °C and 5% CO_2 for 4 h. The resultant structures were examined under an Axiovert 40 CFL inverted phase-contrast microscope (Zeiss, Germany) (at a magnification of 25×). Quantification was carried out in the ImageJ software using the *Angiogenesis Analyzer* package (Carpentier et al., 2020).

2.6. Real-time PCR

For the analysis of gene expression, liver tissue samples were collected near the center of the large lobe. Total RNA was isolated with

the TRIzol reagent. The quality of the RNA was evaluated on a Nanodrop 2000 device (Thermo Fisher Scientific). cDNA was synthesized with the RevertAid First Strand cDNA Synthesis Kit (Thermo Fisher Scientific). To measure the levels of mRNA expression, the following primers were utilized: *Cd31*_F (5′-AGG CAC AAG TGT CTT CCT GG-3′), *Cd31*_R (5′-CGT CTG CAG TGG GCT TAT CT-3′), *Cd34*_F (5′-AGG CTG GGT GAA GAC CCT TA-3′), and *Cd34*_R (5′-GTT GTC TTG CTG AAT GGC CG-3′). The levels of expression of the studied genes were measured relative to *Gapdh* (primers "F" 5′-GAA CAT CCC TGC ATC CAC T-3′ and "R" 5′-ATG CCT GCT TCA CCA CCT TCT T-3′).

The reaction mixture included the EVA Green Master Mix (Synthol, Moscow, Russia). Thermocycling conditions on a CFX96 thermocycler (Bio-Rad, Hercules, USA) were as follows: 2 min initial denaturation at 95 °C and 40 cycles of 10 s at 95 °C (denaturation), 10 s at 60 °C (annealing), and 10 s at 72 °C (elongation). Relative expression levels of the transcripts under study were calculated by the $\Delta\Delta C_t$ method.

2.7. Statistical analysis

The R package *stats* (v.4.3.0) was used to assess statistical significance. First, the data were checked for normality of distribution using the Shapiro-Wilk test. For normally distributed data, significance was evaluated by ANOVA and Tukey's *post-hoc* test for multiple comparisons. For non-normally distributed data, the Kruskal-Wallis test and the pairwise Kruskal-Wallis test adjusted for Benjamini-Hochberg multiple comparisons test or the Wilcoxon test were used.

3. Results

3.1. Gene expression changes

Analysis of differential expression in the liver during *O. felineus* infection revealed 1408 differentially expressed genes (DEGs) (779 overexpressed and 629 downregulated genes). A search for functional enrichment in the set of DEGs using the MSigDB database detected the following terms: signaling events mediated by VEGFR1 and VEGFR2 (P_{adj} = 0.0048), Hallmark_Hypoxia (P_{adj} = 0.012), Hallmark_TGF_Beta_Signaling (P_{adj} = 0.0012), and PDGFR-beta signaling (P_{adj} = 0.000016) (Fig. 1A; Supplementary Table S1). A more detailed analysis of the genes of these pathways indicated that the official gene lists of major pathways overlapped substantially. In particular, Fig. 1A presents a Euler diagram of DEGs ($\log_2$ fold change > 1; P_{adj} < 0.05) in the overlaps among MSigDB hallmarks.

3.2. Abundance of endothelial cell types

To accurately determine endothelial cell type abundance levels from heterogeneous bulk expression data of the liver, we applied the R package *BisqueRNA*. A marker-based method was used that utilizes known cell-specific marker genes to measure relative abundance levels across samples. Based on published scRNA-seq data from the liver (MacParland et al., 2018; Jew et al., 2020), three clusters of endothelial cells were identified. Judging by the expression of their marker genes, these cell clusters were designated as portal endotheliocytes, periportal liver sinusoidal endothelial cells (periportal LSECs), and central venous LSECs. The most abundant was the cluster whose cells were previously described as periportal LSECs (Strauss et al., 2017). They are

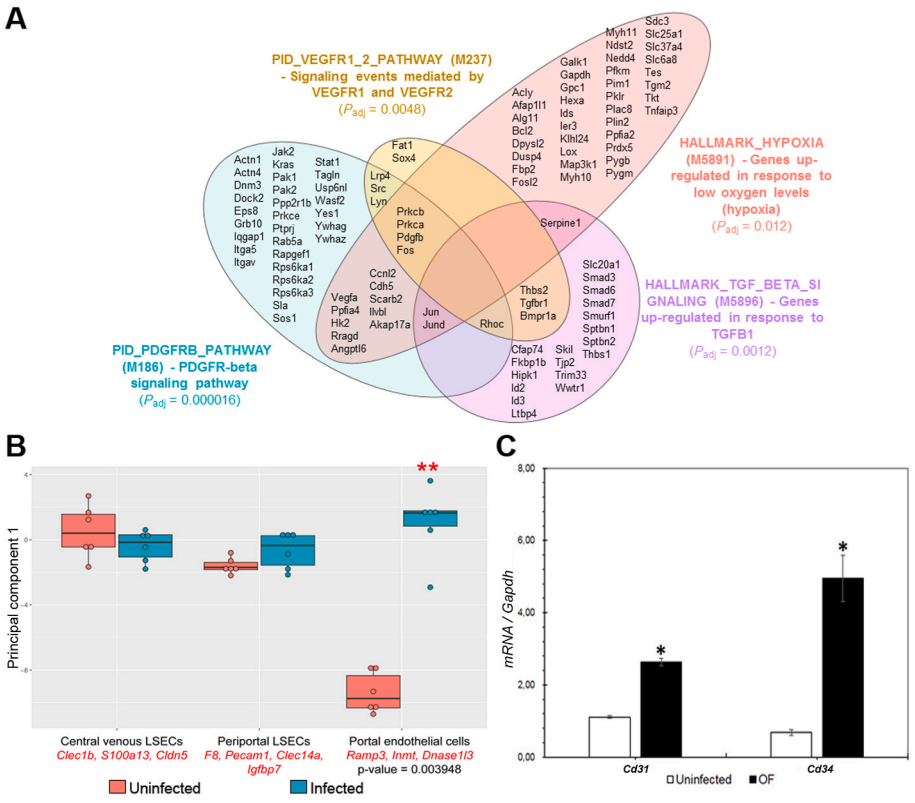

Fig. 1. Identification of signaling pathways associated with the regulation of angiogenesis in the liver of hamsters infected with *Opisthorchis felineus*. **A** Euler diagram illustrating overlaps among the sets of genes matching the enriched MSigDB hallmarks among the DEGs (> 2-fold) in the *O. felineus*-infected hamsters *Mesocricetus auratus*. **B** Box-and-whisker plots of estimated relative cell type abundance levels (principal component 1 values) for endothelial cell markers according to the *BisqueRNA 1.0.5* R-package and human liver scRNA-seq. *Abbreviation*: LSEC, liver sinusoidal endothelial cells. **C** *Cd31* and *Cd34* gene expression in liver tissue of uninfected and *O. felineus*-infected hamsters at one month p.i. as assessed by real-time PCR.

characterized by elevated expression of such markers as *F8*, *Pecam1*, *Sparcl1*, *Tm4sf1*, *Clec14a*, *Id1*, and *Igfbp7*. The second most abundant cluster of endothelial cells was a cluster whose cells are of central venous origin (central venous LSECs) and express *Clec1b*, *S100a13*, *Stab1*, *Gng11*, *Clec4g*, and *Cldn5* as markers. The least abundant cluster was the one that included endothelial cells of the central veins and portal arteries and veins (portal endothelial cells). The markers of these cells are *Ramp3*, *Inmt*, *Dnase1l3*, *Lifr*, *C7*, *Id3*, *Eng*, and *Vwf*.

As compared to controls, a significant endothelial-cell response to infection was observed only for portal endothelial cells (ANOVA with Tukey's correction, $P = 0.004$). No significant response from periportal LSECs and central venous LSECs was observed (Fig. 1B; Supplementary Table S2).

An assay of the expression of endotheliocyte marker genes (*Cd31* and *Cd34*) showed an increase in the expression of these genes one month post-infection, consistent with the general picture of the expression of angiogenesis regulation genes at the transcriptome level (Fig. 1C).

3.3. Histochemistry

Uninfected hamsters showed no amyloid deposition (Fig. 2A). In contrast, amyloid deposition was detected in arteries and veins of various sizes, predominantly in the area of inflammatory infiltrates of the portal triads and in the area of periductal fibrosis in the liver of Syrian hamsters after *O. felineus* infection (Fig. 2B). A similar pattern of amyloid deposition was found in the samples of patients chronically infected with *O. felineus* (Fig. 2C).

3.4. The tube formation assay

EVs were isolated from the worm culture supernatant using a standard protocol. The resulting pellet was confirmed to consist of vesicles of 40–150 nm in size by electron microscopy (Fig. 3A). Elements of the capillary-like network formed by HUVECs were quantified by measurement of the following parameters of pseudo-capillaries *in vitro*: total length of isolated branches, total master segments' length, the number of isolated segments, and the number of meshes (Fig. 3B and C; Supplementary Tables S3 and S4). Judging by the quantification data, both the ESP and EVs stimulated the formation of pseudo-capillaries similarly, by significantly ($P_{adj} < 0.001$) increasing mesh formation (407% and 311%, respectively) and significantly ($P_{adj} < 0.001$) increasing total length of master segments (211% and 183%, respectively). At the same time, the number of isolated segments was reduced by 70% ($P_{adj} = 0.0017$) and 64% ($P_{adj} = 0.0017$) after ESP and EVs treatment, respectively. A similar effect was shown on isolated branches length (reduced by 72% ($P_{adj} = 0.0012$) and 60% ($P_{adj} = 0.0051$) after ESP and EVs, respectively) (Fig. 3B and C). In contrast, BSA, which served as a non-specific control, did not significantly affect any of these parameters. A standard complete endothelial cell culture medium containing all growth factors (Supplementary Fig. S1, Supplementary Table S3) was used as a positive control.

4. Discussion

During the development of tissue- and blood-dwelling helminths, it is apparent that there are direct and indirect interactions with the host's vascular system that initiate proangiogenic events (Dennis et al., 2011). Interactions with the host's vascular system seem to be directly related to processes of fibrogenesis, as confirmed previously by analyses after parasite infection (Hasby Saad and El-Anwar, 2020). For instance, the lung fluke *Paragonimus kellicotti* exhibits early pulmonary pathologies (inflammatory granulomas and fibrosis), which are accompanied by significant alterations of vascularity; this remodeling involves pleural neovascularization, tunica media hyperplasia, and hypertrophy of pulmonary blood vessels and high vascular permeability (Weina and Burns, 1992). Liver infection with *Fasciola hepatica* is characterized by a modification of portal and hepatic veins and hepatic arteries (Shirai et al., 2006). Infection of mice with *Schistosoma mansoni* or *S. haematobium* features inflammatory infiltrates and granulomas surrounding eggs and is coordinated with earlier angiogenesis and later fibrogenesis (Andrade et al., 2006; Botros et al., 2008). The development of inflammatory infiltrates, egg granulomas, and periductal fibrosis within the portal tract of the liver during *O. felineus* infection has also been shown in our previous studies (Pakharukova et al., 2019a, b).

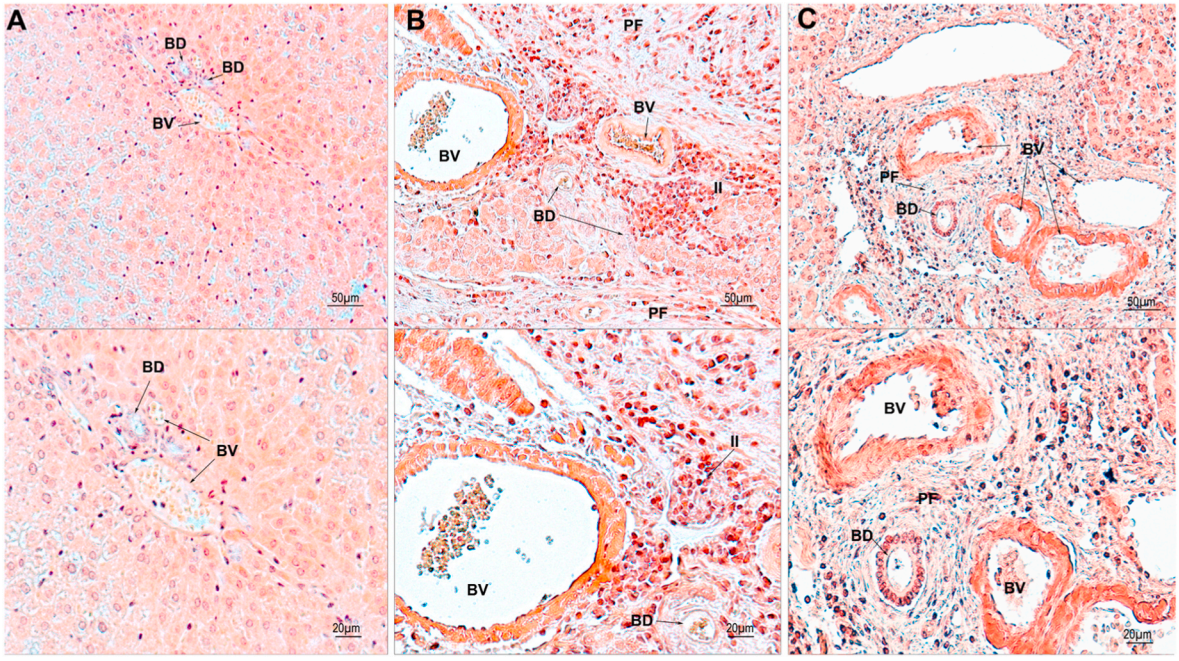

Fig. 2. Congo Red staining of liver samples for the demonstration of amyloid material in vascular walls of uninfected hamster (**A**), *Opisthorchis felineus*-infected hamster at 3 months p.i. (**B**), and in liver tissue section of patient with chronic opisthorchiasis (**C**). Amyloid material is stained orange-red. *Abbreviations*: PF, periductal fibrosis; BD, bile duct; BV, blood vessel; II, inflammatory infiltrate.

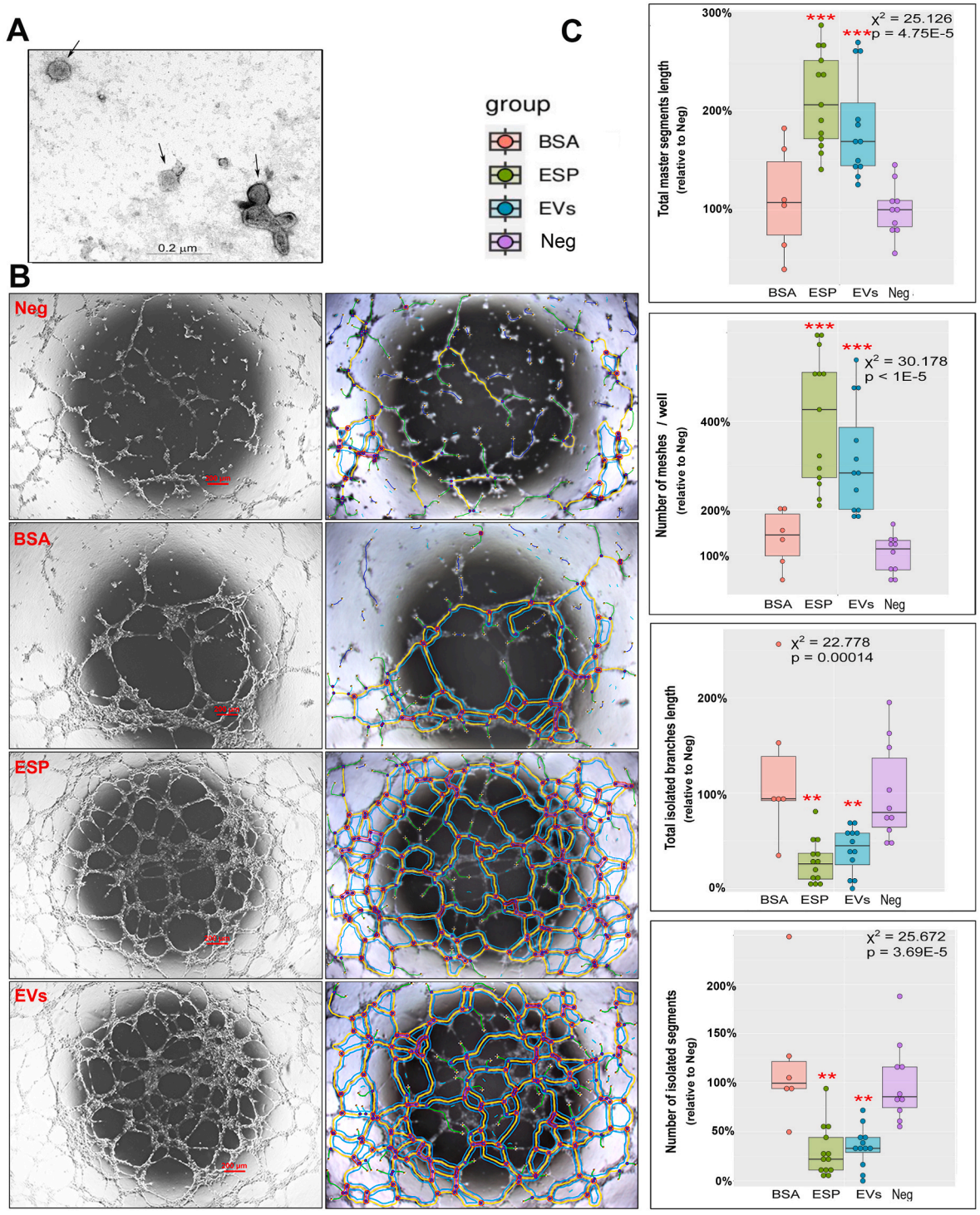

Fig. 3. The ESP and EVs of *Opisthorchis felineus* stimulate angiogenesis. **A** Transmission electron microscopy analysis of EVs derived from *O. felineus*, with an arrow indicating EVs. **B** The endothelial-cell tube formation assay. The right picture panel represents the highlighted tube-formation assay features (meshes are highlighted with cyan, master segments - with yellow, isolated branches - with green, isolated segments - with dark blue, junctions are shown as red dots surrounded in blue). **C** Quantification results of the tube formation assay presented as relative values to the negative control. *Abbreviations*: Neg, negative control; ESP, excretory-secretory product; EVs, extracellular vesicles. *** $P_{adj} < 0.001$; ** $P_{adj} < 0.01$ (as compared to the negative control, pairwise Wilcoxon test with Benjamini-Hochberg correction, Supplementary Table S4).

In this study, at the transcriptome level, we found a significant involvement of portal endothelial cells in the infection. This type of blood vessel is located near portal regions of the liver next to the bile ducts parasitized by the liver fluke. The thickening of the walls of blood vessels and the staining for amyloid that we detected also characterize metabolic changes in the vascular endothelium in opisthorchiasis. Many researchers emphasize the important role of the endothelium of blood vessels as the first cell type to be affected by any kind of liver injury and to orchestrate the liver response to damage; in particular, studies have revealed that aberrant LSEC activation in chronic liver injury induces fibrosis (Lafoz et al., 2020; Gracia-Sancho et al., 2021). Portal (vascular) endothelial cells in the liver respond to damage by acquiring

prothrombotic and antifibrinolytic functions and increased membrane permeability. These functions and properties likely lead to intravascular coagulation, thrombosis and inflammation, and endothelial dysfunction. Amyloid deposits cause the blood vessels to weaken, which can cause their rupture. Hepatic amyloid deposition and its correlation with *S. mansoni* and *S. haematobium* infections have been demonstrated previously (Hamed et al., 2006). In schistosomiasis, vascular distortion and tissue hypoxia precipitated by schistosomal fibrosis have also been observed (Andrade et al., 2006).

Apparently, the pathological changes in blood vessels lead to the emergence of damage-associated molecular patterns (DAMPs). DAMPs in turn activate stellate cells (Lafoz et al., 2020; Gracia-Sancho et al., 2021) and stimulate the production of more angiogenic factors by hepatic satellite cells, thereby also promoting tissue hypoxia and anaerobic glycolysis. These phenomena enhance the production of pyruvate and lactic acid, which are proangiogenic factors (Andrade et al., 2006), just as VEGFA expression (Ferrara et al., 2003). In our set of liver DEGs, we observed significant enrichment with signaling pathways mediated by VEGFR1 and VEGFR2 and with hypoxia, in agreement with literature data. In addition, the formation of the extracellular matrix plays an important part in angiogenesis processes. In the regulation of extracellular-matrix deposition, several signaling cascades are involved, such as the platelet-derived growth factor B (PDGFB) signaling pathway, which participates in the maintenance of microvessels (Jain, 2003), and the TGFβ signaling pathway, which also promotes maturation of blood vessels (Jain, 2003). PDGFB and TGFβ signaling pathways also proved to be significantly enriched within our set of DEGs related to *O. felineus* infection.

There are hypotheses of parasitic helminth-associated angiogenesis postulating that parasites can secrete proangiogenic factors (Dennis et al., 2011). This notion is supported by data on the upregulation of endothelial cell adhesion molecule (ICAM) 1, E-selectin, and vascular cell adhesion molecule (VCAM) 1 during *Schistosoma* egg attachment (Ritter and McKerrow, 1996). Egg-generated, schistosome egg antigen (interleukin-4-inducing principle) is reported to be a proangiogenic growth factor (El-Awady et al., 2001; Mbanefo et al., 2020). Later, it was shown that *S. mansoni*-derived EVs, i.e. exosome-like vesicles and microvesicles, are actively internalized by HUVECs; this phenomenon was accompanied by differential expression of genes regulating vascular endothelial contraction, coagulation, arachidonic acid metabolism, and immune-cell trafficking and signaling (Kifle et al., 2020). The expression of VEGFA, VEGFR2, and mEndoglin and the formation of pseudo-capillaries are significantly enhanced in human vascular endothelial cells treated with a somatic antigen of *Dirofilaria repens* (Pérez Rodríguez et al., 2023). Another example of a parasitic protein that exhibits pro-angiogenic properties may be *O. viverrini* GRN-1 (Haugen et al., 2018), which was found in ESP and captured by host cells (Smout et al., 2009). In our study, we also confirmed that the ESP and EVs of *O. felineus* contain factors that directly stimulate endotheliocytes. It appears that in relation to liver fluke infection, several mechanisms are involved in the regulation of liver vascularization: a release of helminth-derived and/or modification of host-derived proangiogenic factors and an angiogenic switch of endothelial-cell activation. Identification of helminth-derived proangiogenic growth factors in the ESP and EVs is a subject of our next research project.

5. Conclusions

The liver flukes manipulate the host's angiogenic response, which was demonstrated both in an experimental model *in vivo* and during the formation of pseudo-capillaries *in vitro*. The angiogenic activity of helminth secretions is likely one element of the infection-induced pathogenesis. Understanding these pathogenic mechanisms may uncover new therapeutic targets to alleviate or prevent the most severe complications of opisthorchiasis.

Funding

This work was supported by the Russian Science Foundation (grant number 22-24-20010 to MYP). The funding agency had no role in this study, e.g. in study design, data collection, or decision to publish.

Ethical approval

The procedures in this study were in compliance with The Code of Ethics of the World Medical Association (Declaration of Helsinki) for animal experiments (http://ec.europa.eu/environment/chemicals/lab_animals/legislation_en.htm). Syrian hamsters (*Mesocricetus auratus*) were purchased from the specific pathogen-free (SPF) Animal Facility of the ICG SB RAS (RFMEFI61914X0005) (Russia). The hamsters were maintained according to protocols approved by the Committee on the Ethics of Animal Experiments at the Institute of Cytology and Genetics, SB RAS (Permission Number: 25 of December 12, 2014). The Ethics Committee of the Institute of Molecular Biology and Biophysics approved the study of human liver samples and the informed consent form (Protocol #2/2016 of October 27, 2016). The details are presented in Supplementary Text S1). For the experiments with HUVECs, the Ethics Committee of the Institute of Molecular Biology and Biophysics approved the study protocol and informed consent form (Protocol #19 of June 28, 2023). All participants provided written informed consent.

CRediT authorship contribution statement

Dmitry V. Ponomarev: Methodology, Software, Writing - original draft. **Ekaterina A. Lishai:** Methodology, Software, Writing - review & editing. **Anna V. Kovner:** Data curation, Validation, Writing - original draft. **Maria V. Kharkova:** Methodology, Investigation, Writing - original draft. **Oxana Zaparina:** Visualization, Investigation, Writing - review & editing. **Yaroslav K. Kapuschak:** Visualization, Investigation, Writing - original draft. **Viatcheslav A. Mordvinov:** Conceptualization, Writing - review & editing. **Maria Y. Pakharukova:** Conceptualization, Supervision, Software, Writing - review & editing.

Declaration of competing interests

The authors declare that they have no known competing financial interests or personal relationships that could have appeared to influence the work reported in this paper.

Data availability

All data generated or analyzed during this study are included in this published article and its supplementary files.

Acknowledgements

We are thankful to Natalya V. Gubanova for the valuable technical assistance. We are also very grateful to Pavel P. Laktionov for help with reagents. The microscopic analysis was conducted at the Microscopy Center of the ICG SB RAS (No. FWNR-2022-0021; FWNR-2022-0007). The English language was corrected by shevchuk-editing.com. Real-time PCR analysis was conducted at the Center for Collective Use "Proteomic Analysis", supported by funding from the Ministry of Science and Higher Education of the Russian Federation (agreement No. 075-15-2021-691).

Appendix A. Supplementary data

Supplementary data to this article can be found online at https://doi.org/10.1016/j.crpvbd.2023.100153.

References

Andrade, Z.A., Baptista, A.P., Santana, T.S., 2006. Remodeling of hepatic vascular changes after specific chemotherapy of schistosomal periportal fibrosis. Mem. Inst. Oswaldo Cruz 101, 267–272. https://doi:10.1590/s0074-02762006000900041.

Botros, S.S., Hammam, O.A., El-Lakkany, N.M., El-Din, S.H., Ebeid, F.A., 2008. *Schistosoma haematobium* (Egyptian strain): Rate of development and effect of praziquantel treatment. J. Parasitol. 94, 386–394. https://doi.org/10.1645/GE-1270.1.

Carpentier, G., Berndt, S., Ferratge, S., Rasband, W., Cuendet, M., Uzan, G., Albanese, P., 2020. Angiogenesis analyzer for ImageJ - a comparative morphometric analysis of "endothelial tube formation assay" and "fibrin bead assay". Sci. Rep. 10, 11568 https://doi.org/10.1038/s41598-020-67289-8.

Dennis, R.D., Schubert, U., Bauer, C., 2011. Angiogenesis and parasitic helminth-associated neovascularization. Parasitology 138, 426–439. https://doi.org/10.1017/S0031182010001642.

El-Awady, M.K., Gad, Y.Z., Wen, Y., Eassawi, M., Effat, L., Amr, K.S., et al., 2001. *Schistosoma haematobium* soluble egg antigens induce proliferation of urothelial and endothelial cells. World J. Urol. 19, 263–266. https://doi:10.1007/s003450100217.

FAO/WHO, 2014. Multicriteria-based Ranking for Risk Management of Food-Borne Parasites. Microbiological Risk Assessment Series 23. Report of a Joint FAO/WHO Expert Meeting, 3–7 September 2012. Food and Agriculture Organization, Rome, Italy. https://www.fao.org/3/i3649e/i3649e.pdf.

Ferrara, N., Gerber, H.P., LeCouter, J., 2003. The biology of VEGF and its receptors. Nat. Med. 9, 669–676. https://doi.org/10.1038/nm0603-669.

Gracia-Sancho, J., Caparrós, E., Fernández-Iglesias, A., Francés, R., 2021. Role of liver sinusoidal endothelial cells in liver diseases. Nat. Rev. Gastroenterol. Hepatol. 18, 411–431. https://doi.org/10.1038/s41575-020-00411-3.

Hamed, S.M., Kenawy, E.L., A.E, El-Kott, A.F., El-Housini Moustafa, F., Abol-Enein, H., 2006. *Schistosoma*-induced amyloidosis in hamsters is gender-dependent. Int. Urol. Nephrol. 38, 707–712. https://doi.org/10.1007/s11255-006-0055-9.

Hasby Saad, M.A., El-Anwar, N., 2020. Bevacizumab as a potential anti-angiogenic therapy in schistosomiasis: A double-edged, but adjustable weapon. Parasite Immunol. 42, e12724 https://doi.org/10.1111/pim.12724.

Haugen, B., Karinshak, S.E., Mann, V.H., Popratiloff, A., Loukas, A., Brindley, P.J., Smout, M.J., 2018. Granulin secreted by the food-borne liver fluke *Opisthorchis viverrini* promotes angiogenesis in human endothelial cells. Front. Med. 16, 5–30. https://doi:10.3389/fmed.2018.00030.

Jain, R., 2003. Molecular regulation of vessel maturation. Nat. Med. 9, 685–693. https://doi.org/10.1038/nm0603-685.

Jew, B., Alvarez, M., Rahmani, E., Miao, Z., Ko, A., Garske, K.M., et al., 2020. Accurate estimation of cell composition in bulk expression through robust integration of single-cell information. Nat. Commun. 11, 1971. https://doi.org/10.1038/s41467-020-15816-6.

Kifle, D.W., Chaiyadet, S., Waardenberg, A.J., Wise, I., Cooper, M., Becker, L., et al., 2020. Uptake of *Schistosoma mansoni* extracellular vesicles by human endothelial and monocytic cell lines and impact on vascular endothelial cell gene expression. Int. J. Parasitol. 50, 685–696. https://doi:10.1016/j.ijpara.2020.05.005.

Kovner, A.V., Tarasenko, A.A., Zaparina, O., Tikhonova, O.V., Pakharukova, M.Y., Mordvinov, V.A., 2022. Wound healing approach based on excretory-secretory product and lysate of liver flukes. Sci. Rep. 2022 12, 21639. https://doi.org/10.1038/s41598-022-26275-y.

Lafoz, E., Ruart, M., Anton, A., Oncins, A., Hernández-Gea, V., 2020. The endothelium as a driver of liver fibrosis and regeneration. Cells 9, 929. https://doi:10.3390/cells9040929.

Love, M.I., Huber, W., Anders, S., 2014. Moderated estimation of fold change and dispersion for RNA-seq data with DESeq2. Genome Biol. 15, 550. https://doi.org/10.1186/s13059-014-0550-8.

MacParland, S.A., Liu, J.C., Ma, X.Z., Innes, B.T., Bartczak, A.M., Gage, B.K., et al., 2018. Single cell RNA sequencing of human liver reveals distinct intrahepatic macrophage populations. Nat. Commun. 9, 4383. https://doi.org/10.1038/s41467-018-06318-7.

Mbanefo, E.C., Agbo, C.T., Zhao, Y., Lamanna, O.K., Thai, K.H., Karinshak, S.E., et al., 2020. IPSE, an abundant egg-secreted protein of the carcinogenic helminth *Schistosoma haematobium*, promotes proliferation of bladder cancer cells and angiogenesis. Infect. Agents Cancer 15, 63. https://doi.org/10.1186/s13027-020-00331-6.

Mordvinov, V.A., Minkova, G.A., Kovner, A.V., Ponomarev, D.V., Lvova, M.N., Zaparina, O., et al., 2021. A tumorigenic cell line derived from a hamster cholangiocarcinoma associated with *Opisthorchis felineus* liver fluke infection. Life Sci. 15, 119494. https://doi:10.1016/j.lfs.2021.119494.

Pakharukova, M.Y., Mordvinov, V.A., 2016. The liver fluke *Opisthorchis felineus*: Biology, epidemiology and carcinogenic potential. Trans. R. Soc. Trop. Med. Hyg. 110, 28–36. https://doi.org/10.1093/trstmh/trv085.

Pakharukova, M.Y., Mordvinov, V.A., 2022. Similarities and differences among the Opisthorchiidae liver flukes: Insights from *Opisthorchis felineus*. Parasitology 149, 1306–1318. https://doi.org/10.1017/S0031182022000397.

Pakharukova, M.Y., Savina, E., Ponomarev, D.V., Gubanova, N.V., Zaparina, O., Zakirova, E.G., et al., 2023. Proteomic characterization of *Opisthorchis felineus* exosome-like vesicles and their uptake by human cholangiocytes. J. Proteonomics 104927, 283–284. https://doi:10.1016/j.jprot.2023.104927.

Pakharukova, M.Y., Zaparina, O.G., Kapushchak, Y.K., Baginskaya, N.V., Mordvinov, V. A., 2019a. *Opisthorchis felineus* infection provokes time-dependent accumulation of oxidative hepatobiliary lesions in the injured hamster liver. PLoS One 14, e0216757. https://doi.org/10.1371/journal.pone.0216757.

Pakharukova, M.Y., Zaparina, O.G., Kovner, A.V., Mordvinov, V.A., 2019b. Inhibition of *Opisthorchis felineus* glutathione-dependent prostaglandin synthase by resveratrol correlates with attenuation of cholangiocyte neoplasia in a hamster model of opisthorchiasis. Int. J. Parasitol. 49, 963–973. https://doi:10.1016/j.ijpara.2019.07.002.

Pérez Rodríguez, M.D.P., Alarcón-Torrecillas, C., Pericacho, M., Rodríguez-Escolar, I., Carretón, E., Morchón, R., 2023. Effect of somatic antigens of *Dirofilaria repens* adult worms on angiogenesis, cell proliferation and migration and pseudo-capillary formation in human endothelial cells. Parasites Vectors 16, 105. https://doi.org/10.1186/s13071-023-05726-z.

Pozio, E., Armignacco, O., Ferri, F., Gomez Morales, M.A., 2013. *Opisthorchis felineus*, an emerging infection in Italy and its implication for the European Union. Acta Trop. 126, 54–62. https://doi.org/10.1016/j.actatropica.2013.01.005.

Ritter, D.M., McKerrow, J.H., 1996. Intercellular adhesion molecule 1 is the major adhesion molecule expressed during schistosome granuloma formation. Infect. Immun. 64, 4706–4713. https://doi.org/10.1128/iai.64.11.4706-4713.1996.

Scaramozzino, P., Condoleo, R., Martini, E., Bossu, T., Aquilani, S., Spallucci, V., et al., 2018. Behaviour and eating habits as determinants for human opisthorchiasis in the Bolsena Lake area, Italy. Folia Parasitol. 65,, 2018.013. https://doi:10.14411/fp.2018.013.

Shirai, W., Sato, T., Shibuya, H., Naito, K., Tsukise, A., 2006. Anatomicopathological study of vascular and biliary systems using cast samples of *Fasciola*-infected bovine livers. J. Vet. Med. A. Physiol. Pathol. Clin. Med. 53, 239–245. https://doi.org/10.1111/j.1439-0442.2006.00821.x.

Smout, M.J., Laha, T., Mulvenna, J., Sripa, B., Suttiprapa, S., Jones, A., et al., 2009. A granulin-like growth factor secreted by the carcinogenic liver fluke, *Opisthorchis viverrini*, promotes proliferation of host cells. PLoS Pathog. 5, e1000611 https://doi.org/10.1371/journal.ppat.1000611.

Stepanova, A.O., Laktionov, P.P., Cherepanova, A.V., Chernonosova, V.S., Shevelev, G. Y., Zaporozhchenko, I.A., et al., 2019. General study and gene expression profiling of endotheliocytes cultivated on electrospun materials. Materials 12, 4082. https://doi:10.3390/ma12244082.

Strauss, O., Phillips, A., Ruggiero, K., Bartlett, A., Dunbar, P.R., 2017. Immunofluorescence identifies distinct subsets of endothelial cells in the human liver. Sci. Rep. 7, 44356 https://doi.org/10.1038/srep44356.

Weina, P.J., Burns, W.C., 1992. Mortality in Syrian hamsters infected with *Paragonimus kellicotti*. J. Parasitol. 78, 378–380.

Wu, T., Hu, E., Xu, S., Chen, M., Guo, P., Dai, Z., et al., 2021. ClusterProfiler 4.0: A universal enrichment tool for interpreting omics data. Innovation 2, 100141. https://doi:10.1016/j.xinn.2021.100141.

Yu, G., Wang, L.G., Han, Y., He, Q.Y., 2012. ClusterProfiler: An R package for comparing biological themes among gene clusters. OMICS 16, 284–287. https://doi:10.1089/omi.2011.0118.